

# Sensitivity of the deeply bound pionic atoms to the pion-nucleon sigma term $\sigma_{\pi N}$

Natsumi Ikeno,<sup>1,\*</sup> Takahiro Nishi,<sup>2,†</sup> Kenta Itahashi,<sup>2,‡</sup>  
Naoko Nose-Togawa,<sup>3,§</sup> Akari Tani,<sup>1</sup> and Satoru Hirenzaki<sup>4,¶</sup>

<sup>1</sup>*Department of Agricultural, Life and Environmental Sciences, Tottori University, Tottori 680-8551, Japan*

<sup>2</sup>*Nishina Center for Accelerator-Based Science, RIKEN, 2-1 Hirosawa, Wako, Saitama 351-0198, Japan*

<sup>3</sup>*Research Center for Nuclear Physics (RCNP), Osaka University, Ibaraki 567-0047, Japan*

<sup>4</sup>*Department of Physics, Nara Women's University, Nara 630-8506, Japan*

(Dated: April 21, 2022)

We discuss the sensitivity of the observables of the deeply bound pionic atoms to the pion-nucleon sigma term  $\sigma_{\pi N}$  to investigate the possibility of the precise determination of the value of  $\sigma_{\pi N}$  by the accurate data of the deeply bound pionic atoms expected to be obtained at RIBF/RIKEN. We evaluate that the 1 MeV variation of the  $\sigma_{\pi N}$  value  $\Delta\sigma_{\pi N} = 1$  MeV causes the shift of the binding energy  $|\Delta B_{\pi}(1s)| = 5 \sim 7.5$  keV of the  $1s$  pionic atoms in Sn isotopes for the cases considered in this article. The width of the  $1s$  state in the light Sn isotopes has good sensitivity to the  $\sigma_{\pi N}$  value, too. We also study the sensitivity of the formation spectra of the deeply bound pionic atoms to the value of the  $\sigma_{\pi N}$  term. The combined analyses of the observables of the deeply bound pionic atoms are found to be helpful to determine the  $\sigma_{\pi N}$  term precisely. One of the interesting combination of the observables is the energy gap of the  $1s$  and  $2p$  states ( $B_{\pi}(1s) - B_{\pi}(2p)$ ) which experimental error is significantly smaller than that of the absolute value of the binding energy itself of each state. The expected experimental error of the energy gap is  $10 \sim 15$  keV in Sn region which corresponds to the uncertainty of the  $\sigma_{\pi N}$  value around 3 MeV in our evaluation.

## I. INTRODUCTION

Meson-Nucleus systems are known to provide valuable information on the meson properties at finite density [1–4]. Especially, we think spectroscopic study of the deeply bound pionic atoms is very useful to investigate the pion properties [5] and the aspects of the chiral symmetry at finite density [6] based on the theoretical supports [7, 8]. The pion-nucleon sigma term  $\sigma_{\pi N}$ , which is defined as the nucleon matrix element of the mass terms of the light  $u$  and  $d$  quarks in QCD, is one of the essential quantities to investigate the value of the chiral condensate in the nuclear medium. The  $\sigma_{\pi N}$  term is also important to know the contribution of the explicit chiral symmetry breaking to the nucleon mass. The value of  $\sigma_{\pi N}$ , however, has not been determined accurately enough. For example, from the compilation of the  $\sigma_{\pi N}$  values [9, 10] we find that the studies based on the pion-nucleon scattering concluded  $\sigma_{\pi N} \sim 60$  MeV [11–14], while the results by the lattice calculations seems to be distributed within the range of  $\sigma_{\pi N} = 30 \sim 60$  MeV [9, 10, 15–22]. The  $\sigma_{\pi N}$  value determined by the existing pionic atom data is reported to be  $\sigma_{\pi N} = 57 \pm 7$  MeV [23, 24] and is consistent with the results from the  $\pi N$  scattering mentioned above. The analysis of the deeply bound pionic atoms in Ref. [6], on the other hand, indicates the  $\sigma_{\pi N}$  value to be  $\sigma_{\pi N} \sim 45$  MeV, which is in good agreement with

Refs. [25, 26]. In this exploratory level, we are much interested in the determination of the  $\sigma_{\pi N}$  value by the precise data of the deeply bound pionic atoms expected to be obtained in near future [27]. Actually the accuracy of each experimental datum is expected to be improved in coming experiments and we can also make use of the systematic data observed for the long Sn isotopes chain.

The experimental studies of the deeply bound pionic atoms in Sn isotopes have been performed recently at RIBF/RIKEN and the formation spectra of the ( $d, {}^3\text{He}$ ) reaction are measured successfully so that the angular dependence of the spectra is observed first time [28]. The binding energies and widths of the pionic  $1s$  and  $2p$  states have been determined simultaneously with great accuracy. So far, the deeply bound pionic atoms in tin were observed in  ${}^{115}, {}^{119}, {}^{121}, {}^{123}\text{Sn}$  isotopes [6, 28]. Further experimental information with better precision is expected to be obtained for the pionic atoms in  ${}^{111}, {}^{123}\text{Sn}$  by the ( $d, {}^3\text{He}$ ) reaction for  ${}^{112}, {}^{124}\text{Sn}$  targets [27] and it might be very helpful for better determination of the  $\sigma_{\pi N}$  term.

In this article, we discuss the sensitivity of the observables of the deeply bound pionic atoms in  ${}^{111}, {}^{123}\text{Sn}$  to the pion-nucleon sigma term  $\sigma_{\pi N}$  to investigate the possibility of the precise determination of the value of  $\sigma_{\pi N}$  by the accurate data of the deeply bound pionic atoms expected to be obtained at RIBF/RIKEN.

## II. FORMALISM

We explain the theoretical formula here to investigate the structure and formation of the deeply bound pionic atoms. We consider two Models, which indicate two sets

\* ikeno@tottori-u.ac.jp

† takahiro.nishi@riken.jp

‡ itahashi@riken.jp

§ naoko@rcnp.osaka-u.ac.jp

¶ zaki@cc.nara-wu.ac.jp

of the combinations of the pion-nucleus optical potential and the nuclear density distributions, and study the  $\sigma_{\pi N}$  term dependence of the deeply bound pionic atom observables by embedding  $\sigma_{\pi N}$  into the potential parameters.

We solve the Klein-Gordon equation [5, 29],

$$[-\nabla^2 + \mu^2 + 2\mu V_{\text{opt}}(r)] \phi(\vec{r}) = [E - V_{\text{em}}(r)]^2 \phi(\vec{r}), \quad (1)$$

to study the structure of the pionic atoms, where  $\mu$  is the pion-nucleus reduced mass,  $E$  the eigen energy written as  $E = \mu - B_\pi - \frac{i}{2}\Gamma_\pi$  with the binding energy  $B_\pi$  and the width  $\Gamma_\pi$  of the atomic states. The electromagnetic interaction  $V_{\text{em}}$  is described as [30, 31],

$$V_{\text{em}}(r) = -\frac{e^2}{4\pi\epsilon_0} \int \frac{\rho_{\text{ch}}(r') Q(|\vec{r} - \vec{r}'|)}{|\vec{r} - \vec{r}'|} d\vec{r}', \quad (2)$$

here  $Q(r)$  is defined as,

$$Q(r) = 1 + \frac{2}{3\pi} \frac{e^2}{4\pi\epsilon_0} \int_1^\infty du e^{-2m_e r u} \left(1 + \frac{1}{2u^2}\right) \frac{(u^2 - 1)^{1/2}}{u^2} \quad (3)$$

with the electron mass  $m_e$ . This  $V_{\text{em}}$  includes the effects of the finite nuclear charge distribution  $\rho_{\text{ch}}(r)$  and the vacuum polarization.

We consider two combinations of the optical potential  $V_{\text{opt}}$  and the nuclear density distributions (Model (I) and Model (II)), which are explained in the following subsections II A and II B. In the subsection II C, we describe how to embed the  $\sigma_{\pi N}$  term into the optical potential.

We also calculate the pionic atom formation spectra in the ( $d, {}^3\text{He}$ ) reaction with the effective number approach [31–33]. The spectra at the forward angles for the Sn isotopes have been calculated in Ref. [32, 34] and at the finite angles in Refs. [31, 33]. We follow the same formula in this article to calculate the formation spectra.

### A. Model (I)

First, we consider one of the standard optical potential, so called Ericson-Ericson type [35] written as,

$$2\mu V_{\text{opt}}(r) = -4\pi[b(r) + \varepsilon_2 B_0 \rho^2(r)] + 4\pi \nabla \cdot [c(r) + \varepsilon_2^{-1} C_0 \rho^2(r)] L(r) \nabla, \quad (4)$$

with

$$b(r) = \varepsilon_1 [b_0 \rho(r) + b_1 [\rho_n(r) - \rho_p(r)]], \quad (5)$$

$$c(r) = \varepsilon_1^{-1} [c_0 \rho(r) + c_1 [\rho_n(r) - \rho_p(r)]], \quad (6)$$

$$L(r) = \left\{ 1 + \frac{4}{3} \pi \lambda [c(r) + \varepsilon_2^{-1} C_0 \rho^2(r)] \right\}^{-1}, \quad (7)$$

where  $\varepsilon_1$  and  $\varepsilon_2$  are defined as  $\varepsilon_1 = 1 + \frac{\mu}{M}$  and  $\varepsilon_2 = 1 + \frac{\mu}{2M}$  with the nucleon mass  $M$ . The parameters  $b$ 's and  $c$ 's indicate the  $s$ -wave and  $p$ -wave  $\pi N$  interaction, respectively. The parameters  $b_0$  and  $b_1$  are replaced by the density dependent form with the  $\sigma_{\pi N}$  term as explained in subsection II C. The potential terms with parameter  $B_0$  and  $C_0$  are higher order contributions to the optical potential, and  $\lambda$  the Lorentz-Lorenz correction. We use the potential parameters obtained in Ref. [36] except for  $b_0$  and  $b_1$ , which are compiled in Table I.

As for the nuclear densities appeared in the electromagnetic interaction  $V_{\text{em}}$  and the pion-nucleus optical potential  $V_{\text{opt}}$ , we use the Woods-Saxon form in Model (I). The charge density distribution in Eq. (2), which is normalized to the nuclear charge, is written as,

$$\rho_{\text{ch}}(r) = \frac{\rho_{\text{ch}0}}{1 + \exp[(r - R_{\text{ch}})/a_{\text{ch}}]}, \quad (8)$$

with the radius parameter  $R_{\text{ch}}$  and the diffuseness parameter  $a_{\text{ch}}$ . The values of the radius parameter  $R_{\text{ch}}$  are taken from Ref. [37] and shown in Table II. The diffuseness parameter  $a_{\text{ch}}$  in Ref. [37] is fixed to be  $a_{\text{ch}} = t/(4 \ln 3)$  for all nuclei with  $t = 2.30$  fm.

The distributions of the center of nucleon ( $\rho$ ), proton ( $\rho_p$ ), and neutron ( $\rho_n$ ) appeared in Eqs. (4)–(7) are also written by the Woods-Saxon form as,

$$\rho(r) = \rho_p(r) + \rho_n(r) = \frac{\rho_0}{1 + \exp[(r - R)/a]}, \quad (9)$$

where we assume the same distribution shape for the both of the proton and the neutron distributions. The densities  $\rho$ ,  $\rho_p$  and  $\rho_n$  are normalized to be mass, proton and neutron numbers, respectively. The radius and diffuseness parameters  $R$  and  $a$  are determined from the parameters  $R_{\text{ch}}$  and  $a_{\text{ch}}$  of the charge distribution  $\rho_{\text{ch}}$  by the prescription described in Ref. [30].

### B. Model (II)

As for Model (II), we consider the optical potential and the nuclear densities used in the latest analyses of the experimental data of the deeply bound pionic atoms in Sn [38]. The form of the pion-nucleus optical potential  $V_{\text{opt}}$  is modified to have a slightly different imaginary parts from Model (I) as,

TABLE I. Pion-nucleus optical potential parameters used in this article. The parameters for Model (I) are obtained in Ref [36] for the so-called Ericson-Ericson potential [35] and those for Model (II) are obtained in the analyses of the latest experimental data with taking into account the residual interaction effects of the pion and neutron hole [38]. The parameters  $b_0$  and  $b_1$  are determined from the  $\sigma_{\pi N}$  term as discussed in the subsection II C.

Potential parameter	Model (I)	Model (II)
$b_0 [m_\pi^{-1}]$	see subsection II C	see subsection II C
$b_1 [m_\pi^{-1}]$	see subsection II C	see subsection II C
$c_0 [m_\pi^{-3}]$	0.223	0.220
$c_1 [m_\pi^{-3}]$	0.25	0.180
$B_0 [m_\pi^{-4}]$	0.042 $i$	-0.021 + 0.047 $i$
$C_0 [m_\pi^{-6}]$	0.10 $i$	-0.010 + 0.063 $i$
$\lambda$	1.0	1.0

TABLE II. The radius parameter  $R_{\text{ch}}$  of the charge distribution of the Sn isotopes [37] used in Eq. (8) in Model (I). The diffuseness parameter  $a_{\text{ch}}$  in Eq. (8) is fixed to be  $a_{\text{ch}} = t/(4 \ln 3)$  for all nuclei with  $t = 2.30$  fm in Ref. [37].

nuclide	$^{112}\text{Sn}$	$^{124}\text{Sn}$
$R_{\text{ch}}$ [fm]	5.3714	5.4907

$$2\mu V_{\text{opt}}(r) = -4\pi \left[ b(r) + \varepsilon_2 \left( \text{Re}B_0\rho^2(r) + \text{Im}B_0\frac{4}{3}[2\rho_n(r)\rho_p(r) + \rho_p^2(r)] \right) \right] + 4\pi\nabla \cdot \left[ c(r) + \varepsilon_2^{-1} \left( \text{Re}C_0\rho^2(r) + \text{Im}C_0\frac{4}{3}[2\rho_n(r)\rho_p(r) + \rho_p^2(r)] \right) \right] L(r)\nabla, \quad (10)$$

where  $L(r)$  is defined as,

$$L(r) = \left\{ 1 + \frac{4}{3}\pi\lambda \left[ c(r) + \varepsilon_2^{-1} \left( \text{Re}C_0\rho^2(r) + \text{Im}C_0\frac{4}{3}[2\rho_n(r)\rho_p(r) + \rho_p^2(r)] \right) \right] \right\}^{-1}, \quad (11)$$

where the unphysical contributions to the imaginary part of the potential corresponding to the  $\pi^-$  absorption by the neutron pairs are removed out. The form of the  $b(r)$  and  $c(r)$  are the same as those of Model (I). The potential parameters used in Model (II) except for  $b_0$  and  $b_1$  are shown in Table I. The parameters are determined in the analysis of the latest experimental data of the deeply bound pionic atoms in Sn isotopes [38].

In Model (II), we make use of the nuclear densities of Sn isotopes which are determined in Ref. [39]. The measured density distributions are interpolated by the 5-th order Spline function to express the distributions of the center of proton ( $\rho_p$ ) and neutron ( $\rho_n$ ) in the useful form for the analyses of the experimental data [38]. The density functions of odd mass number Sn isotopes are obtained by the interpolation of the averaged data of the nearest neighbor even mass Sn isotopes, e.g.  $^{122}\text{Sn}$  and  $^{124}\text{Sn}$  for  $^{123}\text{Sn}$ . The nuclear distribution  $\rho$  is defined as the sum of the proton and the neutron distributions as  $\rho(r) = \rho_p(r) + \rho_n(r)$ . The nuclear charge distribution  $\rho_{\text{ch}}$  in the electromagnetic interaction  $V_{\text{em}}$  in Model (II) is also obtained and parametrized in the similar manner from the densities determined in Ref. [39]. We consider the pionic atoms only in  $^{123}\text{Sn}$  in Model (II) because of the lack of the experimental information on the estimation of the  $^{111}\text{Sn}$  density at present. The new experiment

has been planned to measure the  $^{112}\text{Sn}$  density distributions [40], which can be used to evaluate the density of  $^{111}\text{Sn}$  reliably. Thus, we can expect to use the  $^{111}\text{Sn}$  density for Model (II) in the near future.

### C. $\sigma_{\pi N}$ term in the optical potential parameters

We consider the pion-nucleus optical potentials in which the  $\sigma_{\pi N}$  term is embedded to study the sensitivities of the observables of the deeply bound pionic atoms to the value of the  $\sigma_{\pi N}$  term. We follow the form proposed in Refs. [41, 42] based on the Tomozawa [43]–Weinberg [44] and the Gell-Mann–Oakes–Renner [45] relations, and determine the value of the  $s$ -wave isovector potential parameter  $b_1$  in terms of  $\sigma_{\pi N}$  as,

$$b_1(\rho) = b_1^{\text{free}} \left( 1 - \frac{\sigma_{\pi N}}{m_\pi^2 f_\pi^2} \rho \right)^{-1}, \quad (12)$$

where  $b_1^{\text{free}}$  is the isovector  $\pi N$  scattering length in vacuum  $b_1^{\text{free}} = -0.0861 m_\pi^{-1}$  [46], and  $f_\pi$  the pion decay constant in vacuum  $f_\pi = 92.4$  MeV [41]. This form is also adopted in Refs. [23, 24].

As indicated in Eq. (12), the  $b_1$  parameter in the potential has the explicit density dependence by including the

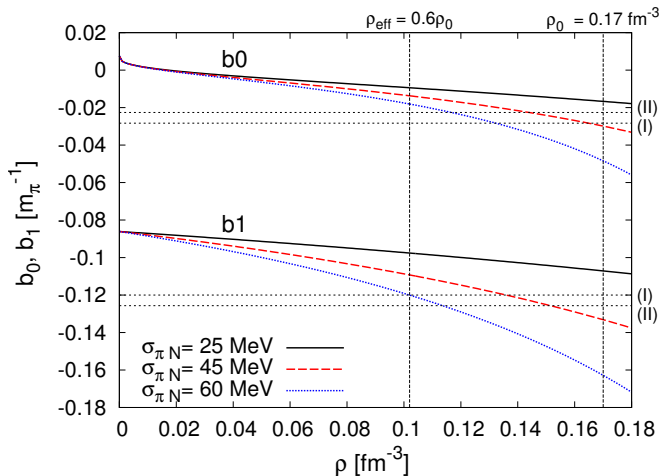


FIG. 1. Density dependence of the  $b_0(\rho)$  (Eq. (13)) and  $b_1(\rho)$  (Eq. (12)) parameters are shown in the figure. The values of the constant  $b_0$  and  $b_1$  parameters in Refs. [36] and [38] indicated as (I) and (II) are also shown by the dotted lines. The normal nuclear density  $\rho_0$  and the effective density  $\rho_{\text{eff}}$  [47] are also indicated in the figure.

$\sigma_{\pi N}$  term. We, then, also take into account the double scattering effects to the  $s$ -wave isoscalar potential parameter  $b_0$  [35] with the density dependent  $b_1$  parameter in Eq. (12) as,

$$b_0(\rho) = b_0^{\text{free}} - \varepsilon_1 \frac{3}{2\pi} (b_0^{\text{free}2} + 2b_1^2(\rho)) \left( \frac{3\pi^2}{2} \rho \right)^{1/3}, \quad (13)$$

where  $b_0^{\text{free}}$  is the isoscalar  $\pi N$  scattering length in vacuum  $b_0^{\text{free}} = 0.0076 m_\pi^{-1}$  [46]. In Eq. (13), the local Fermi momentum of the nucleon is expressed by the nuclear density  $\rho$  as  $\left( \frac{3\pi^2}{2} \rho \right)^{1/3}$ . Thus, the explicit  $\sigma_{\pi N}$  term inclusion requires to consider the density dependent  $b_0$  and  $b_1$  parameters in the optical potential.

### III. RESULTS

In this section, we show the calculated results of the observables of the deeply bound pionic atoms with the different  $\sigma_{\pi N}$  values within the range of  $25 \leq \sigma_{\pi N} \leq 60$  MeV to study the sensitivities of them to  $\sigma_{\pi N}$ .

In Fig. 1, first we show the density dependence of the  $b_0(\rho)$  parameter defined in Eq. (13) and the  $b_1(\rho)$  parameter in Eq. (12) for three different  $\sigma_{\pi N}$  values,  $\sigma_{\pi N} = 25, 45,$  and  $60$  MeV. The normal nuclear density  $\rho_0 = 0.17 \text{ fm}^{-3}$  and the effective density  $\rho_{\text{eff}} = 0.6 \rho_0$  for the pionic atoms, which is introduced in Ref. [47] and used in the analysis of Ref. [6], are indicated in the figure. In Fig. 1, we also plot the constant  $b_0$  and  $b_1$  parameter values obtained in Refs. [36] and [38] for comparison.

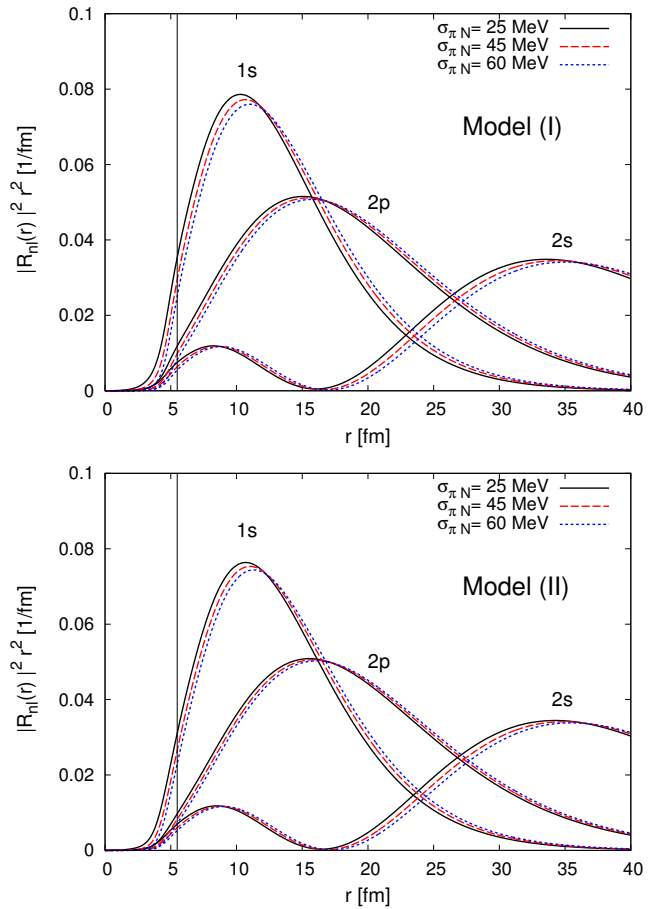


FIG. 2. The radial density distributions of the pionic  $1s$ ,  $2p$ , and  $2s$  states in  $^{123}\text{Sn}$  are plotted as the functions of the radial coordinate  $r$  for the different  $\sigma_{\pi N}$  values as indicated in the figures for Model (I) and Model (II). The density dependent  $b_0(\rho)$  and  $b_1(\rho)$  parameters are used. The vertical line shows the radius of  $^{123}\text{Sn}$ .

The larger  $\sigma_{\pi N}$  values causes the stronger density dependence of the parameters, and thus, causes the more repulsive pion-nucleus  $s$ -wave interaction. We find that the  $b_1(\rho)$  value at the effective density  $\rho_{\text{eff}}$  is almost consistent with the constant  $b_1$  value in Refs. [36] and [38] for the value of  $\sigma_{\pi N} \sim 60$  MeV.

The structures of the deeply bound states are obtained by solving the Klein-Gordon equation with the optical potential Eqs. (4)–(7) for Model (I) and Eqs. (10)–(11) for Model (II). We use the density dependent  $b_0(\rho)$  and  $b_1(\rho)$  instead of the constant  $b_0$  and  $b_1$  values and study how the structure of the states changes with the different values of the  $\sigma_{\pi N}$  term. We show in Fig. 2 the calculated pionic radial density distributions in  $^{123}\text{Sn}$  for Model (I) and Model (II) with the  $b_0(\rho)$  and  $b_1(\rho)$  parameters for  $\sigma_{\pi N} = 25, 45,$  and  $60$  MeV cases. We can see from the figures that the densities are pushed more outwards for the larger  $\sigma_{\pi N}$  values because of the stronger repulsive effects of the potential.

In Fig. 3, the binding energy and the width of the

TABLE III. The calculated average shifts of the observables of the deeply bound pionic states are shown in the unit of keV for the 1 MeV change of the  $\sigma_{\pi N}$  value  $\Delta\sigma_{\pi N} = 1$  MeV.  $\Delta(B_{\pi}(1s) - B_{\pi}(2p))$  and  $\Delta(\Gamma_{\pi}(1s) - \Gamma_{\pi}(2p))$  indicate the average shifts of the differences of the binding energies and widths between the  $1s$  and  $2p$  states for the  $\sigma_{\pi N}$  change  $\Delta\sigma_{\pi N} = 1$  MeV, respectively.

[keV]	$^{123}\text{Sn}$		$^{111}\text{Sn}$
	Model (I)	Model (II)	Model (I)
$ \Delta B_{\pi}(1s) $	6.2	5.0	7.5
$ \Delta\Gamma_{\pi}(1s) $	5.9	4.7	12.9
$ \Delta B_{\pi}(2p) $	1.7	1.4	1.7
$ \Delta\Gamma_{\pi}(2p) $	2.5	1.6	3.6
$ \Delta(B_{\pi}(1s) - B_{\pi}(2p)) $	4.5	3.6	5.8
$ \Delta(\Gamma_{\pi}(1s) - \Gamma_{\pi}(2p)) $	3.4	3.1	9.3

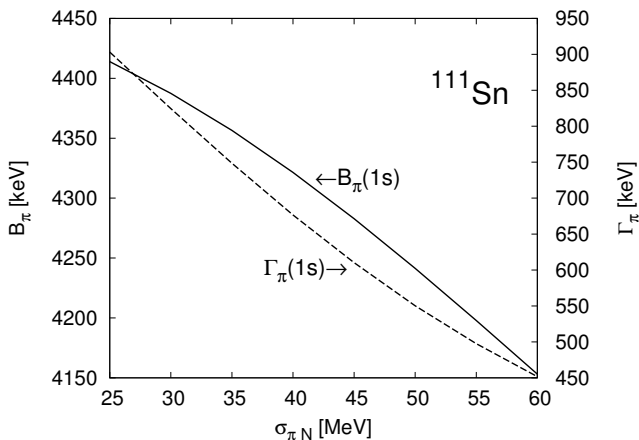


FIG. 3. The binding energy ( $B_{\pi}$ ) and the width ( $\Gamma_{\pi}$ ) of the pionic  $1s$  state in  $^{111}\text{Sn}$  are plotted as the functions of the  $\sigma_{\pi N}$  value for Model (I) with the density dependent  $b_0(\rho)$  and  $b_1(\rho)$  parameters.

deeply bound  $1s$  state in  $^{111}\text{Sn}$  are plotted as the functions of the  $\sigma_{\pi N}$  value for Model (I). In the figure, we find that each observable depends on the  $\sigma_{\pi N}$  value almost linearly within the range of the  $\sigma_{\pi N}$  value considered here. Thus, we use the average slope of the line, namely the average size of the shift of each observable due to the 1 MeV variation of the  $\sigma_{\pi N}$  value  $\Delta\sigma_{\pi N} = 1$  MeV, to express the sensitivity of the observable to  $\sigma_{\pi N}$ . We note here that this figure should not be used directly to determine the  $\sigma_{\pi N}$  value by the binding energy and/or the width since the figure is just to show the sensitivities of the observables to the  $\sigma_{\pi N}$  value. To determine the absolute value of  $\sigma_{\pi N}$ , we need thorough analyses of the data in general. The sizes of the calculated sensitivity of the observables are compiled in Table III for the cases considered in this article. We find that the sensitivities of the  $1s$  state observables are stronger than those of the  $2p$  states as naturally expected and the shifts of the  $1s$  state binding energy  $\Delta B_{\pi}(1s)$  is within the range of  $|\Delta B_{\pi}(1s)| = 5.0 \sim 7.5$  keV for the 1 MeV variation of the  $\sigma_{\pi N}$  value  $\Delta\sigma_{\pi N} = 1$  MeV for the cases considered

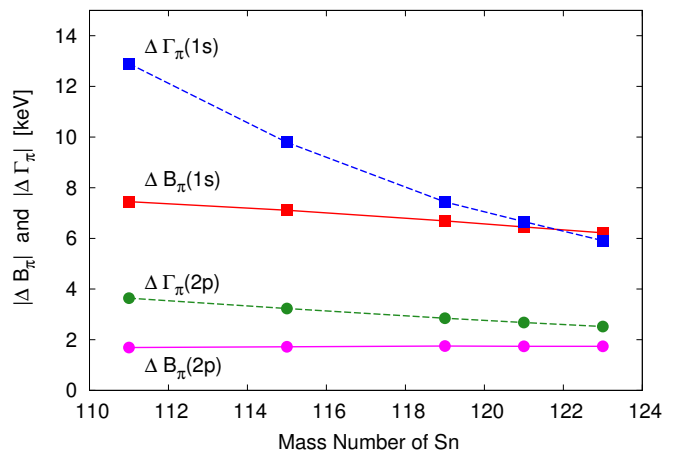


FIG. 4. The mass number dependence of the calculated shifts of the observables of the deeply bound pionic states is shown for the 1 MeV change of the  $\sigma_{\pi N}$  value  $\Delta\sigma_{\pi N} = 1$  MeV in Sn isotopes for Model (I).

here. We also find the larger sensitivities for the pionic states in lighter Sn isotope  $^{111}\text{Sn}$  to  $\sigma_{\pi N}$  because of the less repulsive optical potential due to the smaller neutron numbers and the larger overlap of pionic wave function with nucleus. The shift of the width of the  $1s$  pionic states  $\Delta\Gamma_{\pi}(1s)$  in  $^{111}\text{Sn}$  is 12.9 keV for Model (I) for the  $\Delta\sigma_{\pi} = 1$  MeV variation, which is more than twice of  $\Delta\Gamma_{\pi}(1s)$  in  $^{123}\text{Sn}$  cases as shown in Table III. We show the mass number dependence of the sensitivity of each observable in Fig. 4 and find clearly the stronger sensitivities of the observables, especially  $\Gamma_{\pi}(1s)$ , for lighter Sn isotopes.

These calculated sensitivities of the observables can be compared with the accuracy of the latest experimental data [28, 38]. The typical errors of the up-to-date experiments for the deeply bound pionic atom observables by the  $(d, ^3\text{He})$  reactions in Sn region are around 80 keV for the binding energy of the  $1s$  state and around 40 keV for the width of the  $1s$  state. In addition, some of the combinations of the observables are known to have the advantages to reduce the systematic errors. For our pur-

pose, the gap of the binding energies of the  $1s$  and  $2p$  states,  $B_\pi(1s) - B_\pi(2p)$ , is considered to be important since they can be determined far more accurately and its error is expected to be  $10 \sim 15$  keV for Sn region. We can estimate the uncertainties of the  $\sigma_{\pi N}$  value determination by the expected experimental errors and the calculated sensitivities of the observables. The calculated sensitivity of the energy gap  $|\Delta(B_\pi(1s) - B_\pi(2p))|$  for  $^{111}\text{Sn}$  for Model (I) is 5.8 keV as shown in Table III. In this case, the experimental error  $10 \sim 15$  keV of this energy gap can be interpreted as the uncertainty of the  $\sigma_{\pi N}$  value  $1.7 \sim 2.6$  MeV, which is obtained by dividing the experimental error  $10 \sim 15$  keV by the sensitivity of the observable 5.8 keV for the 1 MeV change of the  $\sigma_{\pi N}$  value. The sensitivities of the energy gap obtained here are 3.6, 4.5, 5.8 keV as shown in Table III. The corresponding uncertainties of  $\sigma_{\pi N}$  to the experimental error  $10 \sim 15$  keV, thus, distribute within the range of  $1.7 \sim 4.2$  MeV. Hence, we evaluate the uncertainty of the  $\sigma_{\pi N}$  value determination using the data of  $|\Delta(B_\pi(1s) - B_\pi(2p))|$  to be around 3 MeV. This is much better than the uncertainties based on the use of the absolute value of  $B_\pi(1s)$  for  $^{111}\text{Sn}$ . The expected size of the experimental error 80 keV of  $B_\pi(1s)$  and the calculated sensitivity 7.5 keV for the 1 MeV change of  $\sigma_{\pi N}$  in  $^{111}\text{Sn}$  conclude that the expected uncertainty of the  $\sigma_{\pi N}$  value is large and would be 11 MeV which is estimated as  $80 \text{ keV} / (7.5 \text{ keV} / \Delta\sigma = 1 \text{ MeV})$ . Similarly, the width of the  $1s$  state for  $^{111}\text{Sn}$  provides the relatively small expected uncertainty of the  $\sigma_{\pi N}$  value to be 3.1 MeV for the experimental error 40 keV. Thus, we find from the typical size of the experimental errors and the calculated sensitivities of the observables that the energy gap between the  $1s$  and  $2p$  states, and the width of the  $1s$  state in lighter Sn isotopes have the larger possibility to provide the important information to determine the  $\sigma_{\pi N}$  value precisely.

Then, we show in Figs. 5–7 the calculated spectra of the  $(d, {}^3\text{He})$  reactions for the formation of the deeply bound pionic states for  $^{112,124}\text{Sn}$  targets for Model (I) and (II) with the density dependent  $b_0(\rho)$  and  $b_1(\rho)$  parameters. We find that the shape of the spectrum have the reasonable sensitivity to the  $\sigma_{\pi N}$  value at each scattering angle. Especially, the peak height of the pionic  $1s$  state formation is clearly reduced for the smaller  $\sigma_{\pi N}$  values for all cases considered here because of the less repulsive potential and thus, larger absorptive width of the state. In the analyses of the experimental formation spectra, we can expect to obtain the information on the potential parameters including the  $\sigma_{\pi N}$  value by comparing them with the theoretical results [28, 38]. As a possibility, the behavior of the shape of the tail of the largest peak structure due to  $1s$  bound state formation could provide the extra information on the  $\sigma_{\pi N}$  value in addition to those from the binding energy and width of the state.

We show in Fig. 8 (left) the calculated angular de-

pendence of the differential cross sections  $\left(\frac{d\sigma}{d\Omega}\right)$  for the pionic  $1s$  and  $2p$  state formation in the unit of the cross section of the elementary process  $d + n \rightarrow {}^3\text{He} + \pi^-$ . The differential cross sections for the specific pionic state formation are obtained theoretically by summing up the contributions of all neutron hole states. We also show the angular dependence of the ratio of the  $1s$  and  $2p$  state formation in Fig. 8 (right) as the similar plot of the experimental data in Fig. 4 in Ref. [28]. We find that the angular dependence of the formation cross section is quite stable to the change of the  $\sigma_{\pi N}$  value and has only rather weak sensitivities to the  $\sigma_{\pi N}$  value.

#### IV. CONCLUSIONS

In this article, we study the sensitivities of the observables of the deeply bound pionic atoms to the value of the pion-nucleon sigma term  $\sigma_{\pi N}$  and investigate the experimental feasibilities of them to determine the  $\sigma_{\pi N}$  value precisely by considering the expected errors of the up-to-date experiments. So far, the analyses of the data have been performed based on the usage of the effective nuclear density  $\rho_{\text{eff}}$  probed by the pionic atoms which would be slightly different for different nuclei and different bound states. In this article, we improve the theoretical formula and implement the  $\sigma_{\pi N}$  term in the optical potential to treat the density dependence of the potential parameters for isoscalar ( $b_0$ ) and isovector ( $b_1$ ) terms explicitly without using the concept of the effective density.

We calculate the various observables and study the sensitivities of them to the  $\sigma_{\pi N}$  value for the deeply bound pionic atoms in  $^{111}\text{Sn}$  and  $^{123}\text{Sn}$  by two Models. We find that the binding energies and widths of the pionic  $1s$  states have the largest sensitivities to the  $\sigma_{\pi N}$  value. The sensitivities tend to be even larger for the lighter Sn isotopes, and the shifts of the  $1s$  binding energy  $\Delta B_\pi(1s)$  and the  $1s$  width  $\Delta\Gamma_\pi(1s)$  in  $^{111}\text{Sn}$  are found to be  $\Delta B_\pi(1s) = 7.5$  keV and  $\Delta\Gamma_\pi(1s) = 12.9$  keV for the variation of the value of the  $\sigma_{\pi N}$  term  $\Delta\sigma_{\pi N} = 1$  MeV. By considering the expected errors of the up-to-date experiments, we conclude that the energy gap of the  $1s$  and  $2p$  pionic states  $|\Delta(B_\pi(1s) - B_\pi(2p))|$  and the width of the  $1s$  state for the lighter Sn isotope are expected to be most important observables to determine the  $\sigma_{\pi N}$  value precisely. The uncertainties to the  $\sigma_{\pi N}$  value due to the experimental errors to these observables are estimated to be 3 MeV. We also find the shapes of the formation spectra by the  $(d, {}^3\text{He})$  reactions have the reasonable sensitivities to the  $\sigma_{\pi N}$  value and we can expect to obtain extra information from the observed spectra by comparing them to the theoretical results.

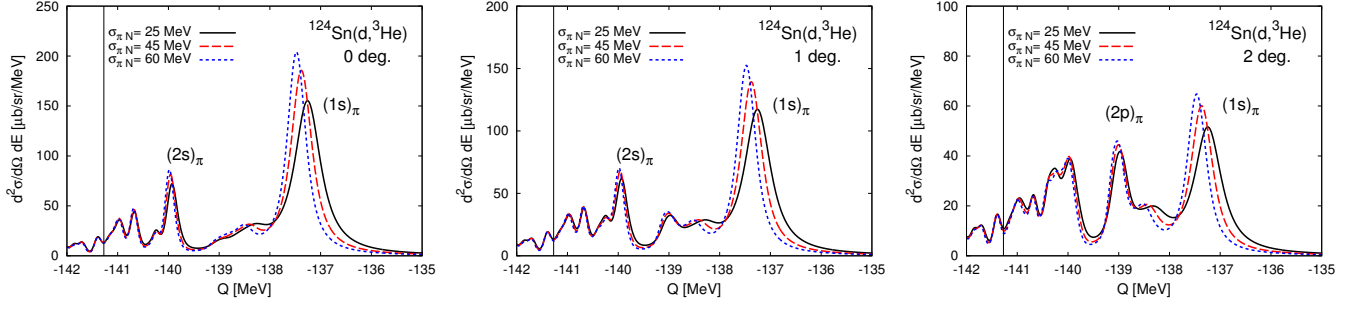


FIG. 5. Formation cross sections of the deeply bound pionic atoms in  $^{123}\text{Sn}$  by the  $^{124}\text{Sn}(d,^3\text{He})$  reactions are shown at the different scattering angles of the emitted  $^3\text{He}$  nucleus in the laboratory frame as  $\theta_{d\text{He}}^{\text{Lab}} = 0^\circ$  (left),  $1^\circ$  (middle),  $2^\circ$  (right), respectively. The results are obtained with Model (I) with the density dependent  $b_0(\rho)$  and  $b_1(\rho)$  parameters with three different  $\sigma_{\pi N}$  values as indicated in the figure. Experimental energy resolution is assumed to be  $\Delta E = 150$  keV. The contributions from the quasi-free pion production are not included in the theoretical spectra.

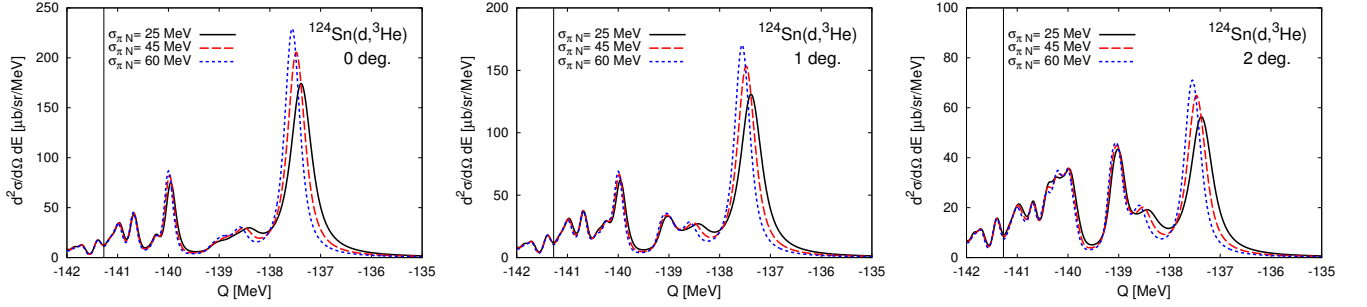


FIG. 6. Same as Fig. 5 except for Model (II) with the density dependent  $b_0(\rho)$  and  $b_1(\rho)$  parameters.

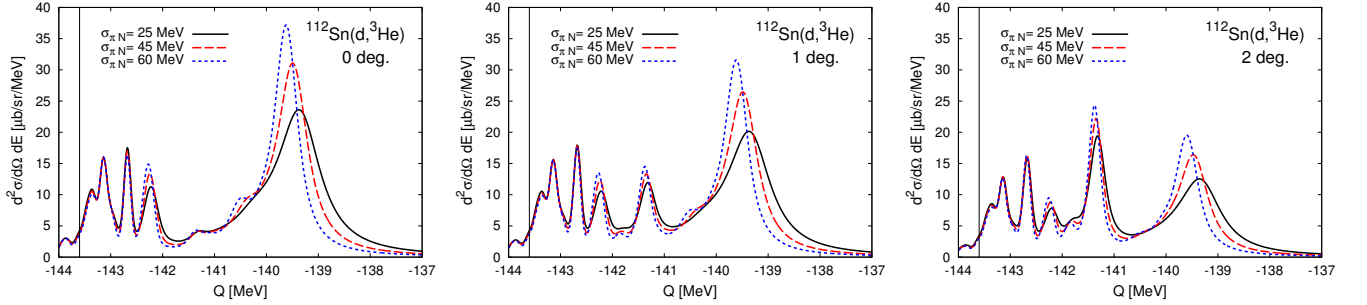


FIG. 7. Same as Fig. 5 except for the deeply bound pionic atoms in  $^{111}\text{Sn}$  by the  $^{112}\text{Sn}(d,^3\text{He})$  reactions.

## ACKNOWLEDGEMENTS

We appreciate the fruitful discussions with D. Jido. The work was partly supported by JSPS KAKENHI Grant Numbers JP19K14709, JP16340083, JP18H01242, JP20KK0070, and by MEXT KAKENHI Grant Numbers JP22105517, JP24105712, JP15H00844.

- [1] C. J. Batty, E. Friedman, and A. Gal, Phys. Rept. **287**, 385 (1997).  
 [2] E. Friedman and A. Gal, Phys. Rept. **452**, 89 (2007).  
 [3] R. S. Hayano and T. Hatsuda, Rev. Mod. Phys. **82**, 2949 (2010).

- [4] V. Metag, M. Nanova, and E. Y. Paryev, Prog. Part. Nucl. Phys. **97**, 199-260 (2017).  
 [5] T. Yamazaki, S. Hirenzaki, R. S. Hayano, and H. Toki, Phys. Rept. **514**, 1-87 (2012).

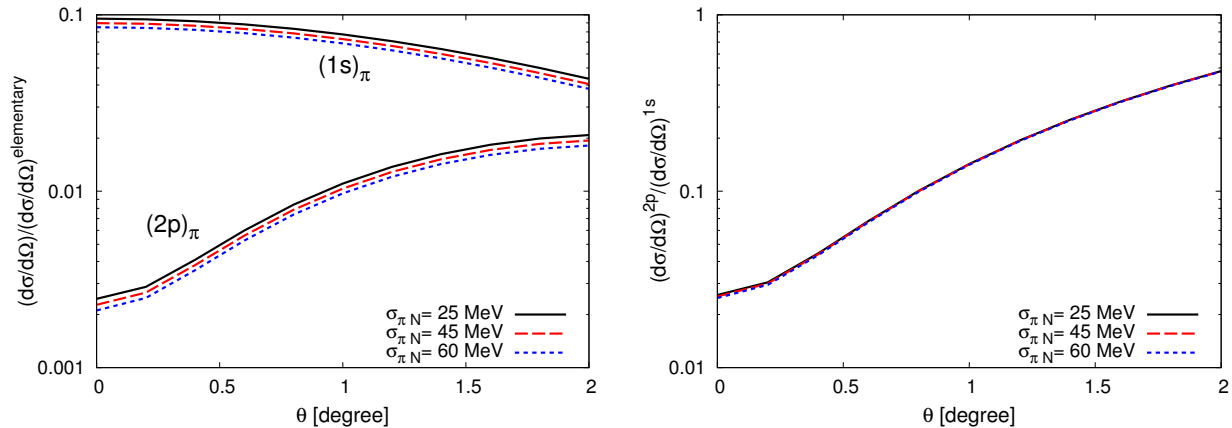


FIG. 8. (Left) The calculated angular dependence of the differential cross sections  $\left(\frac{d\sigma}{d\Omega}\right)$  for the pionic  $1s$  and  $2p$  state formation in the  $^{124}\text{Sn}(d,^3\text{He})$  reaction is shown in the unit of the elementary cross section  $\left(\frac{d\sigma}{d\Omega}\right)^{\text{elementary}}$ . The cross sections are obtained as the sum of the contributions of all neutron hole states, and are calculated with Model (I) with the density dependent  $b_0(\rho)$  and  $b_1(\rho)$  parameters with three different  $\sigma_{\pi N}$  values as indicated in the figure. (Right) The angular dependence of the ratio of the pionic  $1s$  and  $2p$  states formation in the  $^{124}\text{Sn}(d,^3\text{He})$  reaction with Model (I) with the density dependent  $b_0(\rho)$  and  $b_1(\rho)$ .

- [6] K. Suzuki, M. Fujita, H. Geissel, H. Gilg, A. Gillitzer, R. S. Hayano, S. Hirezaki, K. Itahashi, M. Iwasaki, and P. Kienle, *et al.*, Phys. Rev. Lett. **92**, 072302 (2004).
- [7] E. E. Kolomeitsev, N. Kaiser, and W. Weise, Phys. Rev. Lett. **90**, 092501 (2003).
- [8] D. Jido, T. Hatsuda, and T. Kunihiro, Phys. Lett. B **670**, 109-113 (2008).
- [9] N. Yamanaka *et al.* [JLQCD], Phys. Rev. D **98**, 054516 (2018).
- [10] R. Gupta, S. Park, M. Hoferichter, E. Mereghetti, B. Yoon, and T. Bhattacharya, Phys. Rev. Lett. **127**, 24 (2021).
- [11] J. M. Alarcón, J. Martin Camalich, and J. A. Oller, Phys. Rev. D **85**, 051503 (2012).
- [12] D. L. Yao, D. Siemens, V. Bernard, E. Epelbaum, A. M. Gasparyan, J. Gegelia, H. Krebs, and U. G. Meißner, JHEP **05**, 038 (2016).
- [13] M. Hoferichter, J. Ruiz de Elvira, B. Kubis, and U. G. Meißner, Phys. Rev. Lett. **115**, 192301 (2015).
- [14] J. Ruiz de Elvira, M. Hoferichter, B. Kubis, and U. G. Meißner, J. Phys. G **45**, 024001 (2018).
- [15] R. Horsley *et al.* [QCDSF-UKQCD], Phys. Rev. D **85**, 034506 (2012).
- [16] M. F. M. Lutz, R. Bavontaweepanya, C. Kobdaj, and K. Schwarz, Phys. Rev. D **90**, 054505 (2014).
- [17] S. Durr, Z. Fodor, C. Hoelbling, S. D. Katz, S. Krieg, L. Lellouch, T. Lippert, T. Metivet, A. Portelli, and K. K. Szabo, *et al.*, Phys. Rev. Lett. **116**, 172001 (2016).
- [18] X. L. Ren, X. Z. Ling, and L. S. Geng, Phys. Lett. B **783**, 7-12 (2018).
- [19] Y. B. Yang *et al.* [ $\chi$ QCD], Phys. Rev. D **94**, 054503 (2016).
- [20] A. Abdel-Rehim *et al.* [ETM], Phys. Rev. Lett. **116**, 252001 (2016).
- [21] G. S. Bali *et al.* [RQCD], Phys. Rev. D **93**, 094504 (2016).
- [22] C. Alexandrou, S. Bacchio, M. Constantinou, J. Finkenrath, K. Hadjiyiannakou, K. Jansen, G. Koutsou, and A. Vaquero Aviles-Casco, Phys. Rev. D **102**, 054517 (2020).
- [23] E. Friedman and A. Gal, Phys. Lett. B **792**, 340 (2019).
- [24] E. Friedman and A. Gal, Acta Phys. Polon. B **51**, 45-54 (2020).
- [25] J. Gasser, H. Leutwyler, and M. E. Sainio, Phys. Lett. B **253**, 252-259 (1991).
- [26] J. Gasser, H. Leutwyler, and M. E. Sainio, Phys. Lett. B **253**, 260-264 (1991).
- [27] K. Itahashi *et al.*, Proposal for Nuclear Physics Experiment at RI Beam Factory, NP1512-RIBF135 (2019).
- [28] T. Nishi *et al.* [piAF], Phys. Rev. Lett. **120**, 152505 (2018).
- [29] N. Ikeno, R. Kimura, J. Yamagata-Sekihara, H. Nagahiro, D. Jido, K. Itahashi, L. S. Geng, and S. Hirezaki, Prog. Theor. Phys. **126**, 483-509 (2011).
- [30] J. Nieves, E. Oset, and C. Garcia-Recio, Nucl. Phys. A **554**, 509 (1993).
- [31] N. Ikeno, J. Yamagata-Sekihara, H. Nagahiro, and S. Hirezaki, PTEP **2015**, 033D01 (2015).
- [32] Y. Umemoto, S. Hirezaki, K. Kume, and H. Toki, Phys. Rev. C **62**, 024606 (2000).
- [33] N. Ikeno, H. Nagahiro, and S. Hirezaki, Eur. Phys. J. A **47**, 161 (2011).
- [34] Y. Umemoto, Deeply bound pionic atoms – Structure and formation of  $1s$  and  $2p$  states–, Doctoral Thesis, Nara Women’s University (2000).
- [35] M. Ericson and T. E. O. Ericson, Annals Phys. **36**, 323(1966).
- [36] R. Seki and K. Masutani, Phys. Rev. C **27**, 2799 (1983).
- [37] G. Fricke *et al.*, At. Data Nucl. Data Tables **60**, 177 (1995).
- [38] T. Nishi *et al.* [piAF], arXiv:2204.05568 [nucl-ex].
- [39] S. Terashima *et al.*, Phys. Rev. C **77**, 024317 (2008).

- [40] J. Zenihiro, private communication.
- [41] W. Weise, *Acta Phys. Polon. B* **31**, 2715-2726 (2000).
- [42] W. Weise, *Nucl. Phys. A* **690**, 98-109 (2001).
- [43] Y. Tomozawa, *Nuovo Cim. A* **46**, 707-717 (1966).
- [44] S. Weinberg, *Phys. Rev. Lett.* **17**, 616-621 (1966).
- [45] M. Gell-Mann, R. J. Oakes, and B. Renner, *Phys. Rev.* **175**, 2195-2199 (1968).
- [46] V. Baru, C. Hanhart, M. Hoferichter, B. Kubis, A. Nogga, and D. R. Phillips, *Phys. Lett. B* **694**, 473-477 (2011).
- [47] T. Yamazaki and S. Hirenzaki, *Phys. Lett. B* **557**, 20 (2003).